Korean J. Chem. Eng., 37(10), 1773-1785 (2020)
DOI: 10.1007/s11814-020-0572-8

pISSN: 0256-1115
eISSN: 1975-7220

Ion-exchange coupled crystallization for the removal of calcium ions from dicyandiamide

Meiying Huang*,†, Yongsheng Ren, Demin Jiang*, and Junsheng Qi***

*Key Laboratory of Water Environment Evolution and Pollution Control in Three Gorges Reservior (Chongqing Three Georges University), Wanzhou 404100, P. R. China
**School of Chemistry & Chemical Engineering, Ningxia University, Yinchuan 750021, P. R. China
(*Received 14 January 2020 • Revised 9 May 2020 • Accepted 11 May 2020*)

Abstract−A new process for ion exchange coupled crystallization is introduced for the removal of calcium ions from dicyandiamide. The effects of different ion-exchange resins, temperature, reaction time, stirring rate, and treatment amount and resin dosage on the removal of calcium ions in dicyandiamide were studied. On this basis, the crystallization process of dicyandiamide was optimized by response surface methodology, together with respective investigations on the effects of cooling rate, stirring rate, seed grain size and seeding time on the removal of calcium ions in dicyandiamide. It was found that the removal efficiency of calcium ion could reach up to 98.12%, during the ion-exchange treatment, and the value increased then fell, with the rise of stirring rate and temperature; the efficiency would improve, with the accumulation of resin dosage; but it would diminish with the increase of treatment amount; and the value would first rise and then remain unchanged when the reaction time was extended. In addition, the best conditions for crystallization are also provided. When the cooling rate is at 0.3 °C/min, the stirring rate 300 rpm, the seed size 60 meshes, and the seeding time 30 minutes, seeds in uniform size with the content of Ca^{2+} pharmaceutically qualified would be obtained, under the optimum process conditions.

Keywords: Ion Exchange, Dicyandiamide, Calcium Ion, Crystallization, Response Surface Methodology

INTRODUCTION

Dicyandiamide is an important fine chemical material widely used industrially, including pharmaceuticals [1], electronics [2], chronic fertilizer [3,4], and polymer modification [5,6]. With the rapid development of the pharmaceutical, printing and other industries, the demand for high-purity dicyandiamide is increasing, sometimes even bringing about a short supply. At present, the preparation of dicyandiamide mainly adopts the hydrolyzed lime nitrogen method, and the process is as follows. First, CaC_2 reacts with nitrogen to form lime nitrogen and then hydrolyzes the lime nitrogen to form calcium-containing compounds, such as calcium cyanamide. Hereafter, carbon dioxide gas is introduced for decalcification, and the generated cyanamide is concentrated, polymerized and cooled to obtain dicyandiamide products [7]. Due to the incomplete decalcification in the production process, the mother liquor of dicyandiamide crystallization contains $Ca(OH)_2$, $CaCO_3$ and other calcium-containing compounds (such as Ca^{2+}, with a content of about 1,500 mg/kg). These impurities seriously affect the purity and quality of dicyanamide [8]. For the preparation of high-purity dicyandiamide products, it is, therefore, imperative to remove the calcium ions in the dicyandiamide.

By applying different methods, scholars have carried out many fruitful studies on the removal of calcium ions in solution. Silva et al. used chemical precipitation method to remove calcium ions by water feeding from steam generators, and they applied 50 mg/L sodium phosphate to remove calcium ions from water. By their efforts, the maximum removal efficiency reached 81% [9]. Qin et al. synthesized a calcium ion-selective adsorption zeolite that can effectively remove calcium ions from solution. They found that when the pH is 8, the initial calcium concentration of 800 mg/L, the maximum adsorption capacity of calcium achieved 92.35 mg/g, after reacting 70 minutes [10]. Nair and Hwang took the lipophilic ester of phosphoric acid (bis-(2-ethylhexyl) hydrogen phosphate) as a carrier to separate calcium ions from the mixed cationic solution in the solvent of n-dodecane which serves as the supporting liquid film. The results showed that the membrane system can be used as a calcium ion detecting electrode under certain conditions [11]. Marsousi et al. utilized liquid-liquid extraction to extract and recover calcium ions in spiral microchannels. It was found that when operating under optimal conditions, the extraction efficiency of calcium ions was 52%, which was close to the equilibrium extraction efficiency [12]. These methods generally have disadvantages such as large consumption of raw materials, heavy energy consumption, low removal rate, and difficulty in industrial application and promotion, notwithstanding they have reported some progress [9]. Hence, to explore an effective, energy-efficient, simple and easy method to remove calcium ions is extremely urgent and important.

In recent years, a new type of purification and separation technology - ion exchange technology has attracted wide attention [13-16]. Ion exchange technology is a type of chemical reaction that occurs between the isolated and purified ions and exchangers [17].

†To whom correspondence should be addressed.
E-mail: hmytwo@163.com

The technology has been extensively applied in pharmaceuticals [18,19], effluent disposal [20,21], fuel processing [22,23] and other industries, due to its high efficiency, high selectivity, low energy consumption and simple industrial amplification applications. At the same time, some scholars have launched research on the removal of calcium ions in solution, regarding ion exchange technology. Coca et al. used weak cation exchange resin (Lewatit S 8528) instead of strong ion-exchange resin to remove calcium ions in the process of sugar beet production. The study found that the removal rate of calcium ions can surpass 80% [24]. Yu et al. studied the performance of Amberlite IRC 748 resin in removing calcium ions from high concentration potassium chromate solution in a fixed bed column. According to the results, the exchange capacity was reinforced with the increase of initial calcium ion concentration and bed height, but decreased with the increase of flow rate. The research proved that the removal rate of calcium ions under optimal conditions can reach 78.1% [25]. Yi et al. used ion-exchange resin to remove calcium ions from $LiHCO_3$ solution and successfully prepared high-purity Li_2CO_3. Through the exchange process, the removal efficiency of calcium ions was as high as 99.5%, realizing almost complete removal [26]. Although the ion exchange method has been applied to the removal of calcium ions in solutions in some fields, seldom reported is the research of the method for the removal of calcium ions from dicyandiamide crystallization mother liquor.

In view of the excellent characteristics of ion exchange technology for removal of metal ions, we first proposed the use of ion exchange technology to remove the calcium ions in dicyandiamide mother liquor. This method will revolutionize the dicyandiamide purification and impurity removal technology to achieve energy saving, consumption reduction, quality enhancement. On this account, we launched investigation mainly on three aspects. First, the effect of calcium ion removal in dicyandiamide crystallization mother liquor was studied by ion exchange method. Variables including the different types of ion-exchange resin, temperature, reaction time, stirring rate, treatment amount and resin dosage, which may influence the removal of calcium in dicyandiamide, were also researched. In addition, to optimize the crystallization process after the introduction of ion exchange method, we used response surface methodology to study the effects of cooling rate, stirring rate, seed size and crystal growth time on the removal of calcium ions and coefficient of variation (hereinafter referred as CV) in dicyandiamide. This work will help to achieve a breakthrough in the process technology for obtaining high-purity dicyandiamide products and provide guidance for the removal of metal ions by ion exchange.

EXPERIMENTS

1. Materials

Resin (Model: 001x4, 001x7, 001x8 and D001) was purchased from Shanghai Guangnuo Chemical Technology Co., Ltd., disodium edetate from Tianjin Kemiou Chemical Reagent Co., Ltd., calcium carbonate and triethanolamine from Sichuan Xilong Chemical Co., Ltd., sodium hydroxide and hydrochloric acid from Tianjin Guangfu Technology Development Co., Ltd., and anhydrous ethanol from Tianjin Damao Chemical Reagent Factory. All these are analytical reagent, without any further processing. The deionized water (resistivity ≥18.5×104 Ω m) for dissolving solutes was produced by an Aquapro RM-220 (Ever Young Enterprises Development Co., Ltd.). Methyl orange came from Beijing Chemical Works, and the dicyandiamide crystallization mother liquor from Ningxia Dicyandiamide Factory.

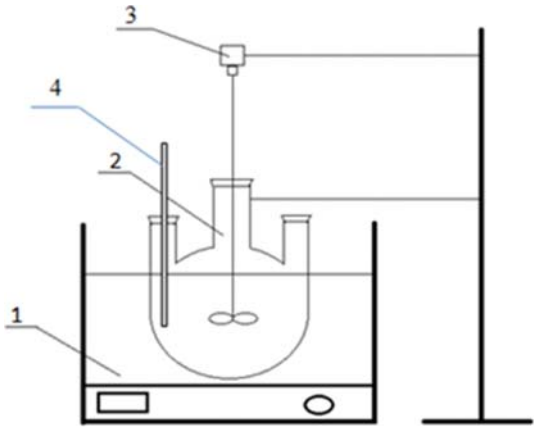

Fig. 1. Experimental setup.
1. Thermostatic heater
2. Three-necked flask
3. Mixer
4. Thermometer

2. Process

The experimental setup is shown in Fig. 1. The setup consists of thermostatic heater, three-necked flask, mixer, and thermometer. The thermostatic heater (DF-101S Zhengzhou Yingyu Yuhua Instrument Co., Ltd.) was used to heat the dicyandiamide crystallization mother liquor. The mixer (BOX-110 Shanghai Specimen Model Factory) was employed to stir the solution. We started from fresh resin cleaning. The fresh resin was pretreated as follows: 40 mL of new resins was placed in a beaker and washed several times with deionized water until the water was clear. Then the resins were soaked with 4% hydrochloric acid solution of about two-times the resins volume for 2 h, and washed with deionized water several times until the pH became between 6 and 7. Subsequently, the resins were soaked with 4% sodium hydroxide solution of about two-times the resin volume for 2 hours. Finally, the pretreated resins were filtered for use. After that, the treated resins and the dicyandiamide crystallization mother liquor to be treated were placed in a three-necked flask as illustrated in Fig. 1. Sequentially, they reacted in a mixer, under an environment of constant temperature by a thermostatic heater. The experimental parameters were as follows: different types of ion-exchange resins (001x4, 001x7, 001x8 and D001), with a temperature of 25-70 °C, reaction time of 5-140 minutes, stirring rate of 10-40 rpm, processing volume of 40-400 mL and resin dosage of 20-65 mL. After the reaction was completed, we measured the content of Ca^{2+} in the dicyandiamide solution before and after the ion exchange by standard solution titration method [9] and calculated the removal rate of the calcium ion by the resins.

The dicyandiamide saturated mother liquor which had gone through the above-described ionic resin exchange treatment was placed in a thermostatic heater. Based on the results of the complete randomized design (one-factor) in the literature, the cooling rate was set at 0.2-0.4 °C/min, the stirring rate was 200-400 rpm, and

the seeds with a mesh of 40-80 were selected. After a seeding time of 20-40 minutes, we adjusted the temperature of the thermostatic water bath and poured the dicyandiamide mother liquor to be crystallized into the three-necked flask [8]. When the temperature dropped to the crystallization metastable zone of the dicyandiamide, seeds were added, and after crystallization were left to grow for a while. Finally, crystals in the crystallizer were filtered and washed several times with absolute ethanol, and then the filtered crystals were naturally dried at the room temperature, and the dried crystals were sieved into a Ziploc bag.

3. Analytical Methods

3-1. Determination of Calcium Ions

Calcium ions were determined by standard solution titration method. The removal efficiency of calcium ions in solution was defined as follows:

$$\eta = \frac{C_0 - C_t}{C_0} \times 100\% \quad (1)$$

where η is the efficiency of calcium ion removal; C_0 is the initial concentration of calcium ions in the solution; C_t is the concentration of calcium ions in the solution at time t.

3-2. C.V Calculation

$$C.V = \frac{100(PD_{84\%} - PD_{16\%})}{2PD_{50\%}} \quad (2)$$

In the formula, $PD_{84\%}$ represents the mesh size, when the accumulated mass fraction under the sieve is 84%; similarly, $PD_{16\%}$ represents the mesh size, when the accumulated mass fraction under the sieve is 16%, and $PD_{50\%}$ represents the mesh size, when the accumulated mass fraction under the sieve is 50%.

3-3. Response Surface Methodology

Response surface methodology has been widely used to optimize experimental schemes or to establish relational models between indicators and factors [27-31]. The principle is to use the multivariate quadratic regression equation to fit the continuous function relationship between the response value and the factor; and to find the optimal parameters by analyzing the regression equation, and to derive the relational surface between all the influencing factors based on the model, thus presenting intuitive options for the optimal area in the experimental design.

In our experiments, four influential factors selected were cooling rate, stirring rate, seed grain size and seeding time. The content of calcium ions in the dicyandiamide crystalline products and the product C.V were set as the response values (Y_1, Y_2). And the four-factor and three-level response surface analytical experiments were implemented. The center point was selected for five times of repeated experiments, for a total of 29 sets of experiments. The process variables and their ranges were determined according to the single-factor experiments and related analysis in our previous work, as shown in Table 1. Thus, a second-order polynomial equation was fitted to correlate the independent variable and the response. The general mathematical form of the second-order polynomial equation is as follows [32]:

$$Y = \beta_0 + \sum_{j=1}^{k} \beta_j X_j + \sum_{j=1}^{k} \beta_{jj} X_j^2 + \sum_{i} \sum_{<j=2}^{k} \beta_{ij} X_i X_j + e_i \quad (3)$$

Table 1. Factor-level

Factor	Level		
	−1	0	1
A Cooling rate (°C/min)	0.2	0.3	0.4
B Stirring rate (rpm)	200	300	400
C Seed size (mesh)	40	60	80
D Seeding time (min)	20	30	40

where Y is the response; β_0 is the model intercept coefficient; X_j and X_i are variables (j and i range from 1 to k); k is the number of independent parameters; β_j, β_{jj} and β_{ij} are interaction coefficients of linear, quadratic and the second-order terms, respectively; and e_i is the error.

After fitting the data to the model, the model was validated and used to construct a 3D response surface contour map to predict the relationship between the independent variable and the dependent variable. In light of these, the work was performed by the Design-Expert [8].

RESULTS AND DISCUSSION

1. Effects of Calcium Ion Removal

1-1. Effect of Ion-exchange Resin Type and Treatment Amount

Fig. 2 displays the efficiency of Ca^{2+} removal from the dicyandiamide crystallization mother liquor, by presenting the performance of four distinct types of ion-exchange resins and with different treatment amount, where the temperature (45 °C), time (30 minutes), stirring rate (250 rpm), resin dosage (40 mL) are specifically conditioned. It was found that the 001×7 ion-exchange resin reported the highest Ca^{2+} removal efficiency in the dicyandiamide crystallization mother liquor. Hence, the 001×7 ion exchange resin was employed in all of the subsequent studies. Experimental results also revealed that with the increase of the treatment amount, the removal efficiency of Ca^{2+} in the dicyandiamide crystallization mother liquor of all types of ion-exchange resins decreased gradually. One expla-

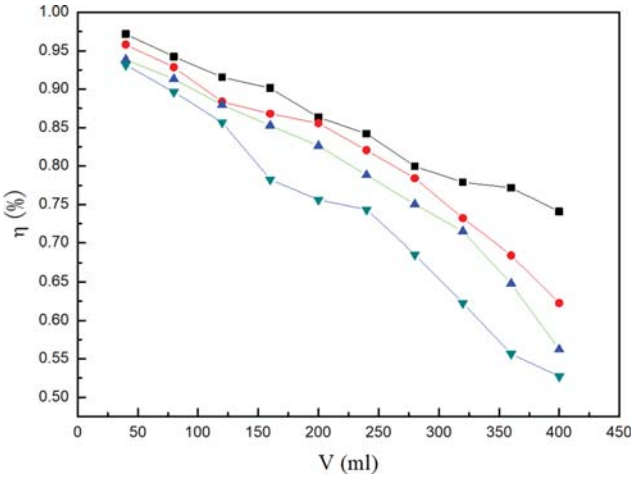

Fig. 2. Effects of the four types of resins and treatment amount on decalcification (■, 001×7; ●, 001×8; ▲, 001×4; ▼, D001).

nation is that as the amount of treatment increases, the effect of ion-exchange resin on Ca^{2+} removal reaches saturation, which in turn leads to a gradual decline in the removal efficiency of Ca^{2+}.

1-2. Effect of Ion-exchange Resin Treatment Amount

Fig. 3 shows the effect of ion-exchange resin on the removal of Ca^{2+} in 200 mL dicyandiamide crystalline mother liquor at 45 °C for 30 minutes and with a stirring rate of 250 rpm. It can be seen from Fig. 3 that in the investigated range of the amount of ion-exchange resin, as the amount of resin increases, the adsorption amount of Ca^{2+} per unit volume of resin gradually decreases; besides, the removal rate of Ca^{2+} increases. As shown, when the amount of resins varies within the range of 20-30 mL, the removal rate of Ca^{2+} increases rapidly and the slope of the curve changes sharply. Regarding of the treatment effect, when the amount of resins comes to 40 mL, the removal rate of Ca^{2+} has reached 90.0%; when the amount of resins exceeds 40 mL, the slope of the curve becomes smaller, and the removal rate of Ca^{2+} exhibits a trend of slower growth. Then when the amount of resins is 50 mL, the removal rate of Ca^{2+} can reach 94.25%, with the concentration of calcium ions of 83 mg/kg. At this time, the calcium content has reached the industry requirement for pharmaceutical grade dicyandiamide on calcium content. Thereafter, the removal rate tends to grow slightly, whereas the amount of the resin is continuously increased. However, from the economic point of view, the greater the amount of resins consumed, the higher the processing cost. Therefore, considering the high-quality dicyandiamide industry requirements and the removal rate of Ca^{2+}, the optimal choice of ion-exchange resin lies in the range of 40-50 mL in the process of the experiment.

1-3. Effect of Temperature

Fig. 4 shows the effect of temperature on the removal of Ca^{2+} in the 200 mL of dicyandiamide crystalline mother liquor, where the ion-exchange resin (40 mL), reaction time (30 minutes) and stirring rate (250 rpm) are specifically conditioned. According to the picture, as the temperature increases from 25 to 45 °C, the removal efficiency of calcium ions rises from 95.08 to 98.12%; when the temperature is within the range of 45-50 °C, the removal efficiency of calcium ions reaches the maximum. But when the temperature increases in the range of 50-70 °C, the removal efficiency of calcium ions drops from 97.99% to 95.52%. One possible reason behind the ups and downs within the investigated temperature range might

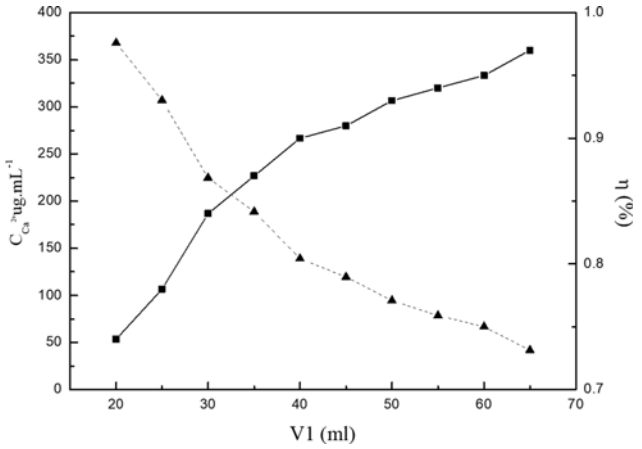

Fig. 3. Effect of resin dosage on decalcification (▲, concentration of calcium ions; ■, extraction rate).

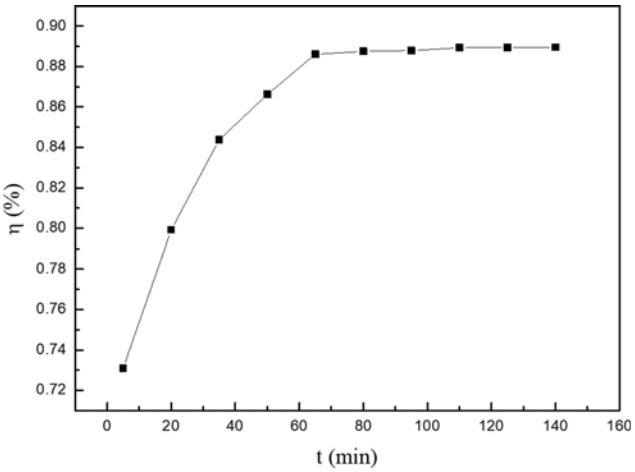

Fig. 5. Effect of time on Ca^{2+} removal rate.

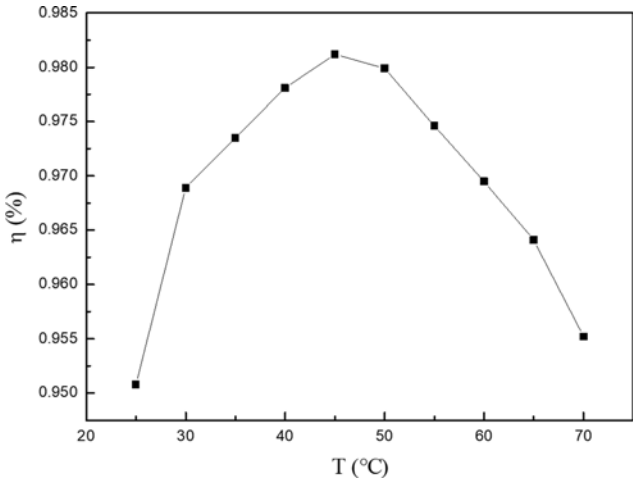

Fig. 4. Effect of temperature on Ca^{2+} removal rate.

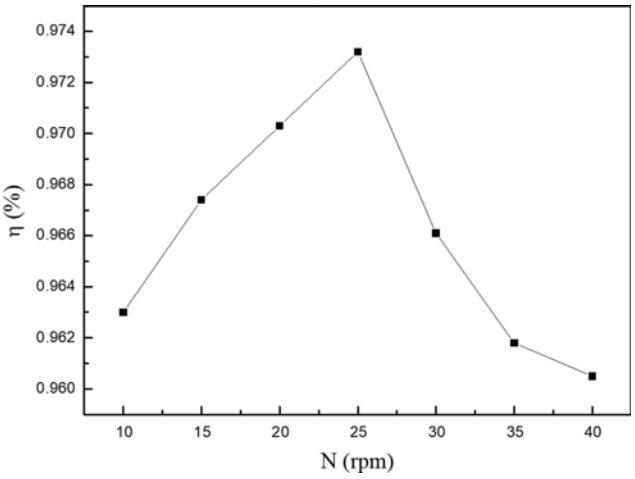

Fig. 6. Effect of stirring rate on decalcification.

be that when the temperature rises, the viscosity of the solution decreases, and the random movement of calcium ions in the mother liquid is aggravated, so that the concentration of calcium ions in the solution is distributed more evenly. Meanwhile, the liquid film between the two phases becomes thinner, which accelerates the rate of ion exchange between calcium ions and the resins [33]. On the other hand, when the temperature is too high, the structure of the resin would be destroyed, then its capability of exchange is deprived, finally resulting in the decline of lower selectivity on calcium ions and further the decrease of removal efficiency. Therefore, it is preferred to select an exchange temperature within 45-50 °C in the process of the experiment.

1-4. Effect of Time

Fig. 5 manifests the effect of reaction time on the removal of Ca^{2+} in the 200 mL of dicyandiamide crystalline mother liquor, where the ion-exchange resin (40 mL), stirring rate (250 rpm) and temperature (45 °C) are specifically conditioned. We found that with the extension of the exchange time, the removal efficiency of Ca^{2+} increased. To be specific, when the reaction time extends in the range of 0-40 minutes, faster growth of removal efficiency occurs, compared with that of performance in the time range of 40-70 minutes. What may account for the rapid growth rate and the later slower growth rate is that Ca^{2+} mainly reacts with the surface of resin at the beginning of ion exchange, and the constant stirring could facilitate the ion diffusion between the resin surface and the crystalline mother liquid. As the ion exchange reaction proceeds, the concentration of Ca^{2+} which has not ion exchanged in the mother liquor gradually decreases. And at the same time, when the surface exchange of the resin reaches saturation, Ca^{2+} starts to move along the pores of the resin toward the inside of the resin. Since some of the internal pores of the resin are clear, some with one of the end closed, the diffusion resistance of the resin to calcium ions in the solution is strengthened, thereby reducing the ion exchange rate. When the exchange time exceeds 70 minutes, the ion exchange reaches a balance, and the exchange between the resins and the calcium ions in the mother liquor realizes a saturated state. In this case, if the saturated resin is not taken out timely, it is possible that the exchanged calcium ions return to the mother liquor, which

Table 2. Experimental design and results of Y_1 and Y_2 models

No.	Cooling time (°C/min)	Stirring rate (rpm)	Seed grain size (mesh)	Seeding time (min)	Content of calcium ions (Y_1)		Coefficient of variation (Y_2)	
					Experimental value	Predicted value	Experimental value	Predicted value
1	0.2	400	60	30	43.96	43.53	0.66	0.65
2	0.3	300	60	30	30.63	32.74	0.51	0.53
3	0.4	300	60	40	34.47	35.48	0.55	0.55
4	0.3	300	40	20	24.91	22.79	0.47	0.44
5	0.3	400	60	40	45.58	45.69	0.68	0.67
6	0.4	400	60	30	41.25	39.53	0.63	0.61
7	0.2	300	60	20	24.40	26.96	0.44	0.47
8	0.3	200	60	40	24.55	24.63	0.46	0.46
9	0.3	300	60	30	31.99	32.74	0.52	0.53
10	0.3	400	80	30	47.73	48.62	0.69	0.71
11	0.3	300	60	30	32.83	32.74	0.53	0.53
12	0.3	300	60	30	33.25	32.74	0.53	0.53
13	0.4	300	80	30	41.25	40.57	0.62	0.61
14	0.3	200	60	20	14.42	12.47	0.34	0.34
15	0.2	300	40	30	36.43	35.27	0.56	0.56
16	0.2	200	60	30	21.65	21.64	0.43	0.43
17	0.3	300	60	30	34.99	32.74	0.55	0.53
18	0.2	300	60	40	40.47	40.39	0.60	0.61
19	0.4	300	60	20	21.40	25.04	0.42	0.45
20	0.3	300	40	40	39.38	37.87	0.59	0.57
21	0.3	200	80	30	26.80	27.31	0.48	0.48
22	0.4	200	60	30	20.14	18.83	0.41	0.40
23	0.3	400	40	30	36.83	39.89	0.57	0.60
24	0.2	300	80	30	41.79	40.90	0.64	0.62
25	0.4	300	40	30	29.72	28.77	0.50	0.49
26	0.3	300	80	40	43.07	43.45	0.65	0.65
27	0.3	400	60	20	35.91	33.99	0.56	0.55
28	0.3	200	40	30	15.93	18.61	0.39	0.41
29	0.3	300	80	20	34.86	34.65	0.55	0.54

allows the exchange process to achieve a dynamic balance.

1-5. Effect of Stirring Rate

Fig. 6 shows the effect of stirring rate on the removal of Ca^{2+} in the 200 mL of dicyandiamide crystalline mother liquor, where the ion-exchange resin (40 mL), reaction time (30 minutes) and temperature (45 °C) are specifically conditioned. It was found that when the stirring speed rose from 100 to 250 rpm, the calcium ion removal rate grew with the increase of the stirring rate in the process of calcium ion removal from the dicyandiamide crystalline mother liquor. It indicates that in the range of appropriate stirring rate, an intensified removal rate of calcium ions can be realized by boosting the stirring rate. This is because the increase of the stirring rate can attenuate the thickness of liquid film between the resins and the mother liquor, which is favorable for the mass transfer in the mother liquor. As the stirring rate increases during the ion exchange process, the liquid film becomes thinner, leading to the acceleration of the diffusion process of the liquid film. When the stirring rate reaches 250 rpm, the removal rate of calcium ions achieves a maximum of 97.35%, the thickness of the liquid film is smallest, and the influence of the stirring rate on the speed of ion exchange lessens. When the stirring speed is greater than 250 rpm, the calcium ion removal rate of the resins in the mother liquor decreases as the stirring rate increases. The result verifies that the stirring rate has an important influence on the performance of calcium ion removal. When speeding up stirring, the flow resistance of the exchanged solution grows, which hinders the mass transfer process of calcium ions in the mother liquor. Yet, a relatively large stirring rate may intensify the friction and mechanical collision between the ion-exchange resins as well. It may even break the resin, then the mechanical loss of the resin increases, weakening its exchange performance. As a result, the production cost would increase. Accordingly, a stirring rate of about 250 rpm registers a desirable performance of calcium ions removal with deliberation of cost-effectiveness.

2. Optimized Crystallization Process by Response Surface Methodology

2-1. Mathematical Model

According to the BBD design, the results are shown in Table 2. We carried out two different tests on the experimental data in Table 2, namely, total square sum and model summary statistics, regression models between various models. The results, as shown in Appendix A, demonstrate that the quadratic model used to predict the dicyandiamide crystallization process is appropriate. The experimental results were analyzed by multiple regression analysis, and the relation between the independent variables and the response was expressed by a second-order polynomial equation. Based on the above analysis, a regression equation model of two response values of calcium ion content and coefficient of variation was established [34]. The two code-conversed regression equations are as

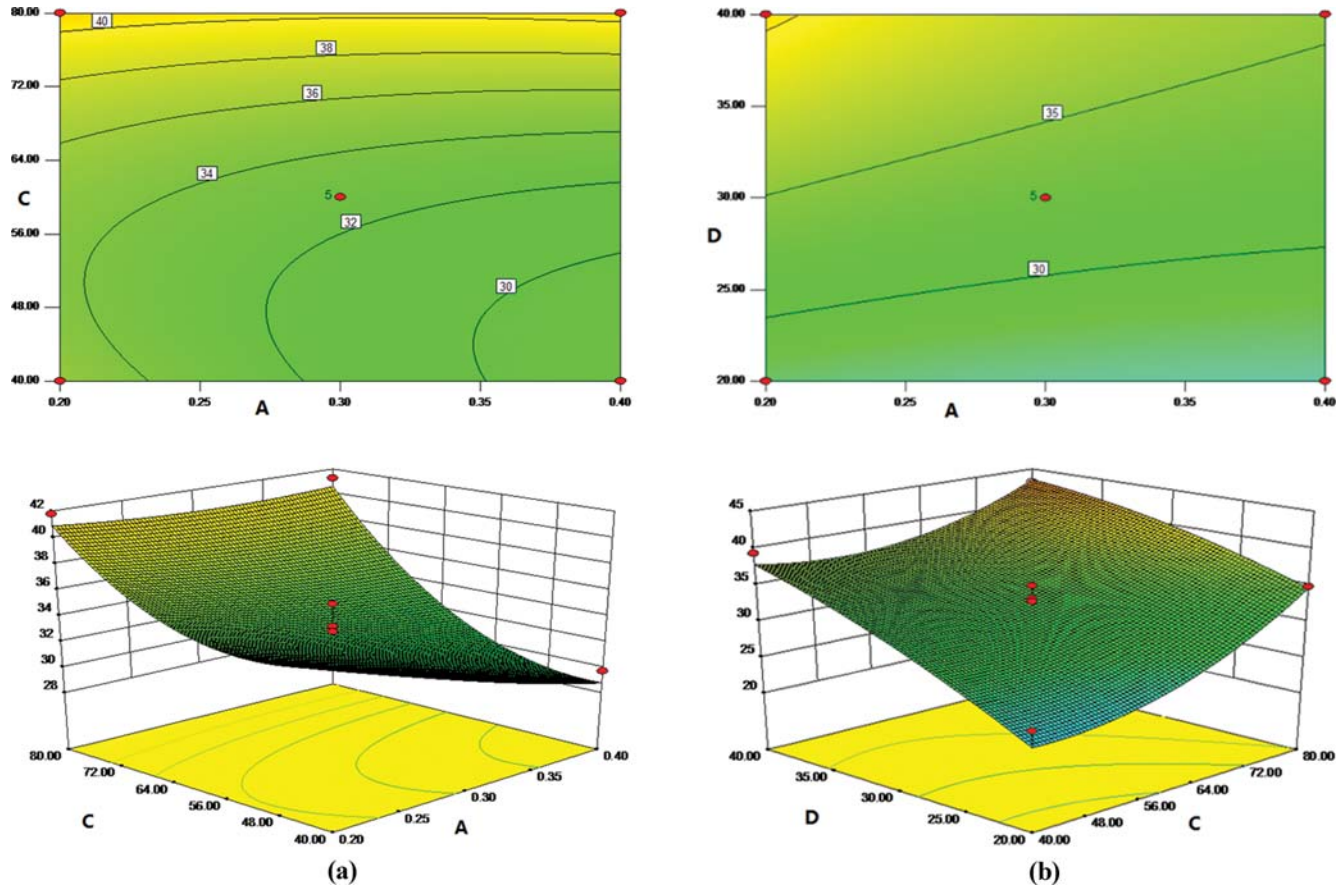

Fig. 7. (a) Interaction between cooling rate and seed grain size; (b) interaction between cooling rate and seeding time; (c) interaction stirring rate interacts with seed grain size; (d) interaction between seed grain size and seeding time.

follows:

$$Y_1 = -34.83 - 59.35833A + 0.25752B - 0.73383C + 2.06383D - 0.03AB + 0.77125AC - 0.75AD + 0.00000375BC - 0.000115BD - 0.007825CD + 45.875A^2 - 0.00231375B^2 + 0.00795C^2 - 0.0123D^2$$

$$Y_2 = +0.12528 - 0.48587A + 0.00169113B - 0.011312C + 0.01803D - 0.0004325AB + 0.005575AC - 0.009375AD + 0.0000047875BC + 0.00000075BD - 0.000021875CD + 0.64283A^2 - 0.00000135717B^2 + 0.0000926958C^2 - 0.000134217D^2$$

Subsequently, the sufficiency of the above mathematical model was evaluated by constructing a diagnostic map, and the results are shown in Appendix B. It can be seen from Appendix B that when comparing the experimental values with the predicted values in the figure, the predicted values of the Y_1 model and the Y_2 model are consistent with their experimental results.

2-2. Effect of Process Variables

On the basis of 3.2.1, the cooling rate, stirring rate, seed grain size and seeding time were plotted as the response values of calcium content and the C.V of grain size in dicyandiamide crystalline products, which can visualize the interaction between various factors. The changed color from blue to green in the Fig. 7 indicates that the response value becomes larger. And the shape of the contour line can reflect the degree of interaction between factors. The closer the shape is to a circle, the less the interaction between factors; while the closer the shape is to an oval, the more active is the interaction.

The contour line and response surface map of model Y_1 are shown in Fig. 7. In Fig. 7(a), with the stirring rate conditioned at 300 rpm and the seeding time of 30 minutes, the interaction between the cooling rate and the grain size is remarkable. When the size of the added seeds is less than 48 meshes, the concentration of calcium ions and the rate of calcium ion removal diminish with the increasingly dropping temperature rate. When the size is greater than 48 meshes, the concentration of calcium ion and the rate of calcium ion removal witness a decline as the cooling rate increases. But, in this case, the decline tends to be slower. In Fig. 7(b), with the stirring rate conditioned at 300 rpm and the grain size of 60 meshes, the interaction between the cooling rate and the seeding time is not significant. When the temperature drops in a range of 0.2-0.4 °C/min, the concentration of calcium ions gradually increases with the seeding time rising from 20 to 40 minutes. The reason for the strengthened concentration may be that the extension of the seeding time leads to some seeds dissolving, resulting in an increase in the concentration of calcium ions. In Fig. 7(c), with the cooling rate conditioned at 0.3 °C/min and the seeding time of 30 minutes, the interaction between the stirring rate and the grain size is not evident. When the stirring rate ranges from 200 to 400 rpm, the concentration of calcium ions reduces, as the grain size decreases. In Fig. 7(d), with the stirring rate conditioned at 300 rpm and the drop rate of temperature at 0.3 °C/min, the interaction between the seeding time and the seed grain size is notable. In the case where the grain size reaches a certain value and the seeding time increases

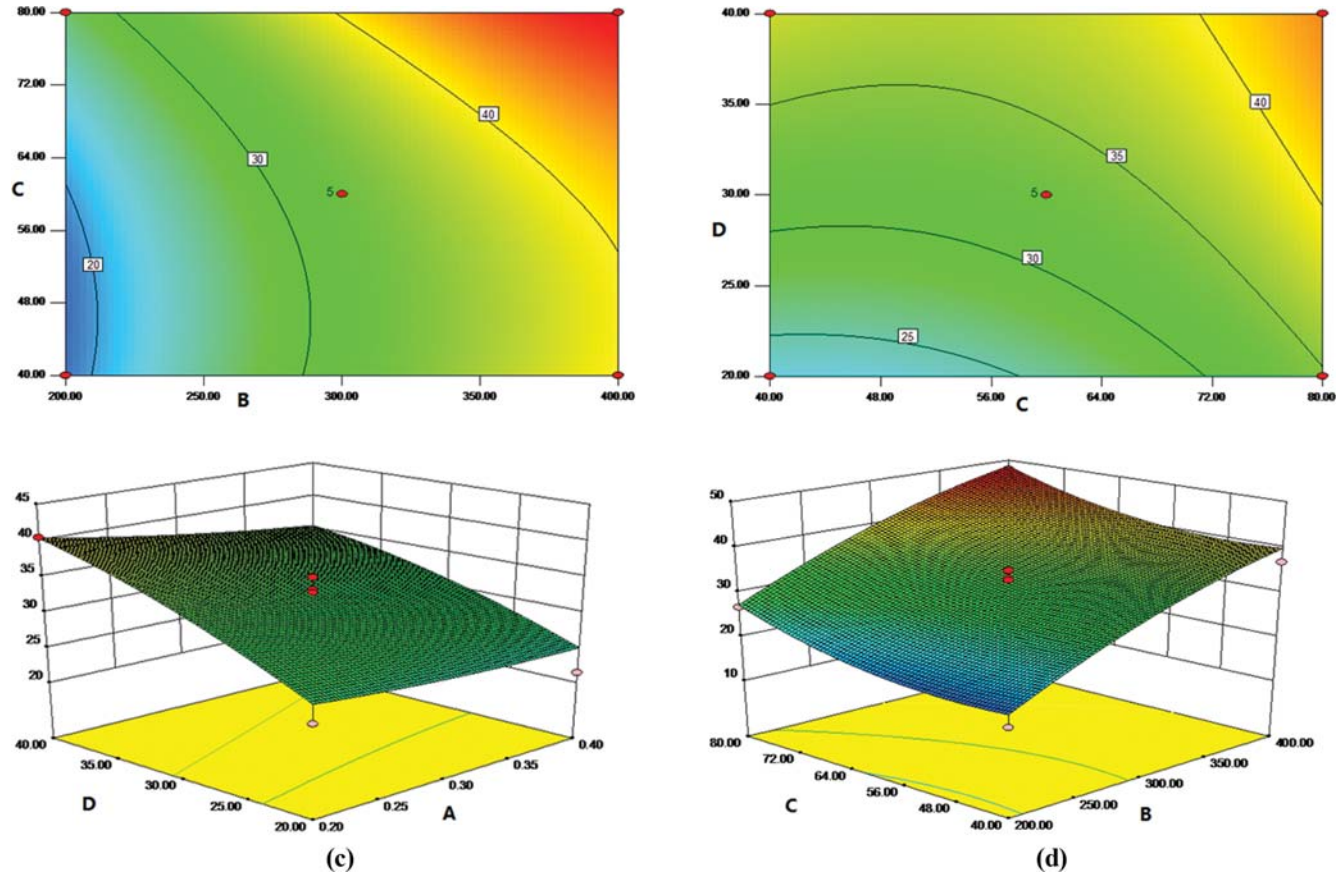

Fig. 7. Continued.

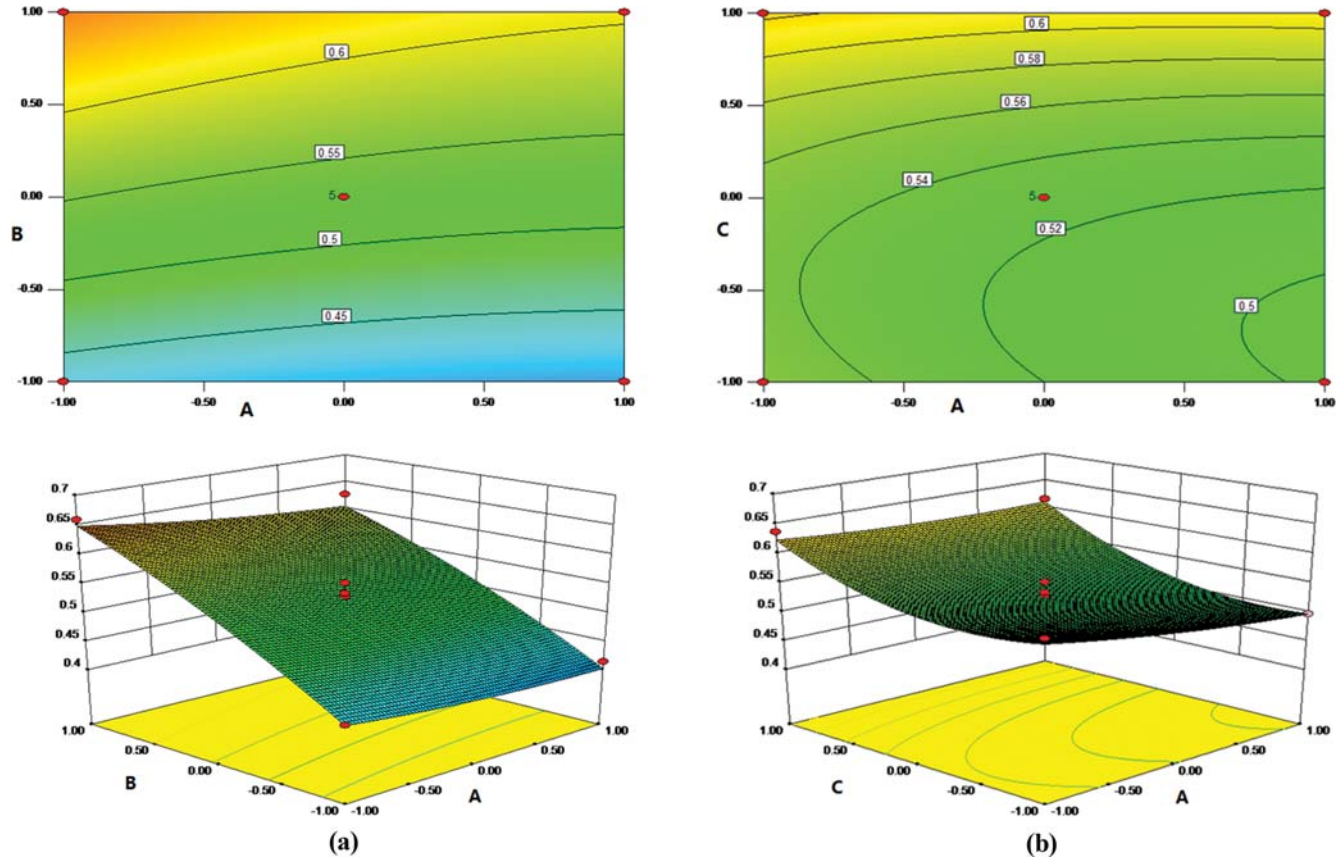

Fig. 8. (a) Rate of cooling and the interaction of the stirring rate; (b) interaction between cooling rate and seed size; (c) interaction between cooling rate and seeding time; (d) interaction stirring rate interacts with seed grain size; (e) interaction between cooling rate and seeding time; (f) interaction between seed grain size and seeding time.

from 20 to 40 minutes, the concentration of calcium ions drops as the seeding time decreases.

The contour line and response surface map of model Y_2 are shown in Fig. 8. In Fig. 8(a), the interaction between the cooling rate and the stirring rate is not strikingly noticeable, with the seeding time conditioned for 30 minutes and the seed grain size of 60 meshes. When the cooling rate rises from 0.2 to 0.3 °C/min, the coefficient of variation gradually increases and shows a faster growth, as the stirring rate enlarges from 200 to 300 rpm. And when the cooling rate rises from 0.3 to 0.4 °C/min, the coefficient of variation gradually increases yet shows slower growth, as the stirring rate rises from 300 to 400 rpm. In Fig. 8(b), the interaction between the cooling rate and the grain size is significant, with the stirring rate conditioned at 300 rpm and the seeding time of 30 minutes. When the cooling rate is less than 0.25 °C/min, the coefficient of variation decreases slowly with the decrease of the grain size. When the cooling rate is greater than 0.25 °C/min and the grain size is in the range of 40-50 meshes, the coefficient of variation decreases with the decrease of the grain size. And the turning point is when the seed grain size is in the range of 50 to 80 meshes and the coefficient of variation increases as the grain size declines. In Fig. 8(c), the interaction between the cooling rate and the seeding time is not so perceptible, with the stirring rate conditioned at 300 rpm and the seed grain size of 60 meshes. When the cooling rate increases from 0.2 to 0.4 °C/min, the coefficient of variation goes up, as the seeding time increases from 20 to 40 minutes. In Fig. 8(d), the interaction between the stirring rate and the grain size is intense, with the cooling rate conditioned at 0.3 °C/min and the seeding time of 30 minutes. When the stirring rate is less than 0.25 °C/min, the coefficient of variation gradually decreases with the decrease of grain size. When the stirring rate is greater than 0.25 °C/min and the grain size increases from 40 to 50 meshes, the coefficient of variation decreases accordingly as the grain size decreases. But when the grain size rises from 50 to 80 meshes, the coefficient of variation increases as the grain size decreases. In Fig. 8(e), the interaction between the cooling rate and the seeding time is not prominent, with the stirring rate conditioned at 300 rpm and the seed grain size of 60 meshes. When the cooling rate goes from 0.2-0.4 °C/min, the coefficient of variation increases with the extension of seeding time from 20 to 40 minutes. In Fig. 8(f), the interaction between the seeding time and the grain size is conspicuous, with the cooling rate conditioned at 0.3 °C/min and the stirring rate of 300 rpm. When the seed grain size is less than 50 meshes and the seeding time ranges from 20-40 minutes, the coefficient of variation shows a slow increase as the seeding time extends. When the grain size exceeds 50 meshes and the seeding time ranges from 20-40 minutes, the coefficient of variation decreases, as the grain size decreases.

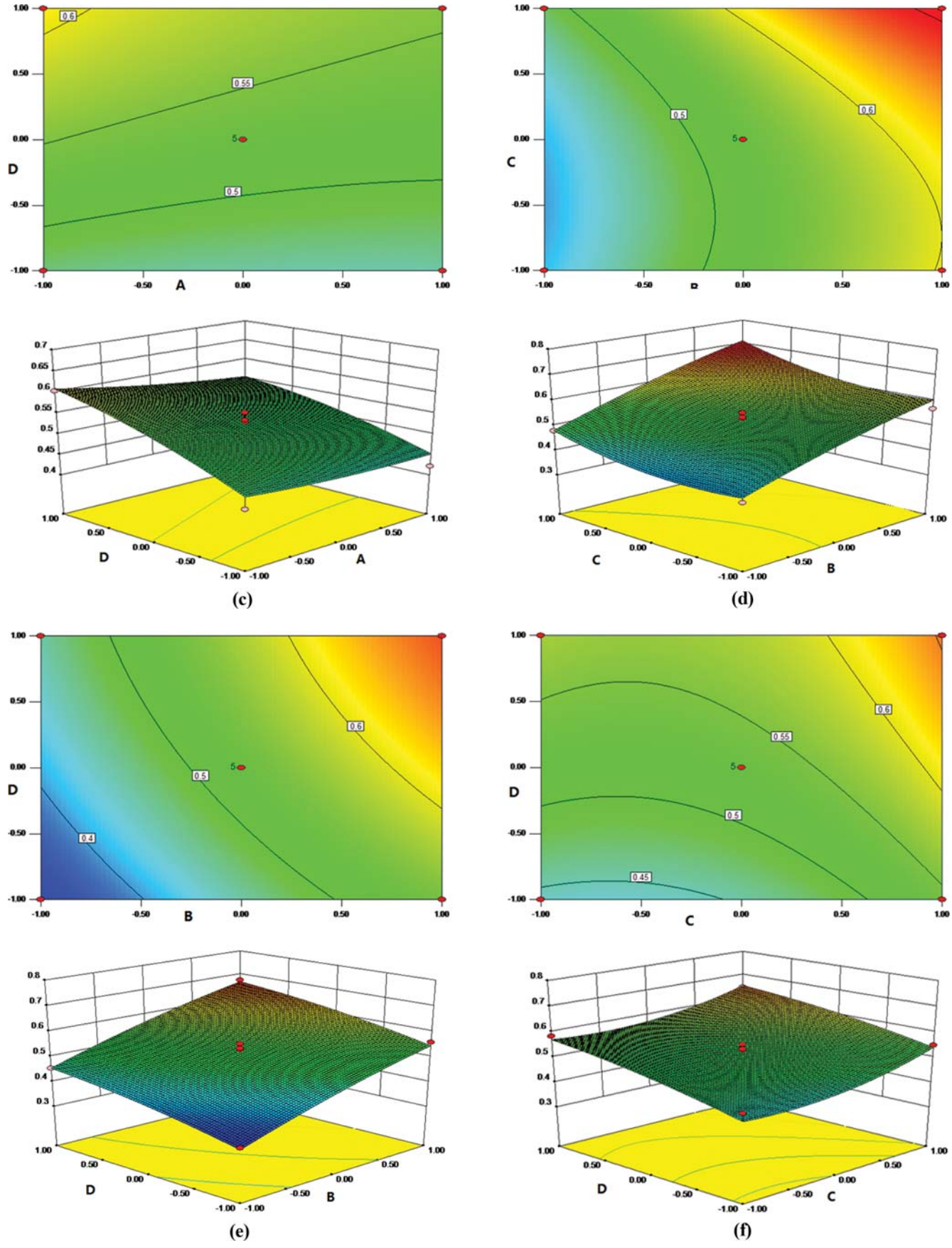

Fig. 8. Continued.

Table 3. Optimization results of the dicyandiamide crystallization

Optimized target	Cooling rat (°C/min)	Stirring rate (rpm)	Seed grain size (mesh)	Seeding time (min)
$Y_{1(min)}$	0.3	300	60	30
$Y_{2(min)}$	0.2	400	80	40

2-3. Optimization

The optimization calculations were carried out by the prediction models of Y_1 and Y_2, and the crystallization process of the two models was obtained as shown in Table 3. Provided to taking either Y_1 or Y_2 alone as an optimized target, a contradictory result would occur. This is because the rate of cooling is a driving force for seeding, and a relatively high stirring rate and long seeding time would break seeds. Additionally, the selection of rather small grain size of seeds can enlarge the specific surface area and correspondingly bring more seeding points, thus accelerating the seeding rate. With this regard, we chose Y_1 as the main optimized objective and considered Y_2 should not be too large. From Table 3, it is evident that in order to obtain dicyandiamide crystals with uniform grain size and comparatively little calcium ions, the optimum process conditions are determined as a cooling rate of 0.3 °C/min, a stirring rate of 300 rpm, a seed grain size of 60 meshes, and a seeding time of 30 minutes. Under such condition, dicyandiamide crystals in uniform grain size and with the calcium ion concentration of 32.29 mg/kg would be obtained.

CONCLUSIONS

We have proposed a new method for the removal of ion-exchange coupled crystallization of calcium ions in dicyandiamide mother liquor. We also studied the effects of different ion-exchange resins, reaction time, temperature, treatment amount, stirring rate and resin dosage on the calcium ion removal in dicyandiamide. According to the experimental results, during the ion-exchange treatment, when the stirring rate and temperature increased and then decreased, the amount of resins increased and the amount of treatment increased, and the reaction time increased first and then remained unchanged; under optimal experimental conditions, the highest efficiency of calcium ion removal was 98.12%. On this basis, the crystallization process of dicyandiamide was optimized by response surface methodology, regarding the investigations on the effects of cooling rate, seed size, stirring rate and seeding time on calcium ion removal in dicyandiamide, respectively. It was found that when the cooling rate was optimally conditioned at 0.3 °C/min, the stirring rate at 300 r/min, the grain size at 60 meshes and the seeding time of 30 minutes, the seed grain sizes were uniform and the Ca^{2+} removal rate would hit 98.35%, which meets the requirements on the content of Ca^{2+} in pharmaceutical grade dicyandiamide products. In the future, further studies on the mechanism of the intrinsic action of ion-exchange resin to remove calcium ions from dicyandiamide mother liquor are expected to be conducted.

ACKNOWLEDGEMENT

This work was supported by the Youth project of science and technology research program of Chongqing Education Commission of China (KJQN201901208).

NOMENCLATURE

C_0 : initial concentration of calcium in solution [mg/kg]
C_t : concentration of calcium in solution at time t [mg/kg]
C.V : variable coefficient
D : seed grain size [mesh]
e_i : error value
k : number of independent parameters
N : stirring rate [rpm]
R : cooling rate [°C/min]
PD : mesh size of the accumulated mass fraction under the screen
T : temperature [°C]
t : reaction time [min]
t1 : seeding time [min]
V : volume of dicyandiamide crystal mother liquor [mL]
V1 : volume of resin [mL]
X : variable
Y : response value

Greek Letters

β_0 : model intercept coefficient
β_j : interaction coefficients of linear
β_{jj} : quadratic term
β_{ij} : the second-order term
η : removal efficiency of calcium ions [%]

REFERENCES

1. E. S. Khalil, B. Saad, E. M. Negim and M. I. Saleh, *J. Polym. Res.*, **22**, 116 (2015).
2. R. Zhang, L. Liu, J. Zhang, W. Y. Wang, F. Ma, R. F. Li and L. Z. Gao, *J. Solid State Electrochem.*, **19**, 1695 (2015).
3. X. Y. Zhang, G. Qian, X. Y. Yang, C. L. Hu and X. G. Zhou, *Fluid Phase Equilib.*, **363**, 228 (2014).
4. P. Pal, A. M. S. McMillan and S. Saggar, *Biol. Fertil. Soils*, **52**, 539 (2016).
5. J. B. Liu, Y. Wang, S. S. Tang, Q. Gao and R. F. Jin, *New J. Chem.*, **41**, 13370 (2017).
6. Y. X. Ma, D. Xing, C. P. Lu, X. Y. Du and P. Q. La, *Polym. Compos.*, **39**, 2232 (2018).
7. J. G. Gao and L. M. Zhao, CN Patent, 102320994A (2012).
8. X. F. Guo, *Research on removal of calcium ion by ion exchange*, Ningxia University Publications, Ningxia (2017).
9. R. D. R. Silva, R. T. Rodrigues, A. C. Azevedo and J. Rubio, *Environ. Technol.*, **40**, 1 (2019).
10. C. H. Qin, R. Wang and W. Ma, *Desalination*, **259**, 156 (2010).
11. S. G. Nair and S. T. Hwang, *J. Membr. Sci.*, **64**, 69 (1991).
12. S. Marsousi, J. Karimi-Sabet, M. A. Moosavian and Y. Amini, *Chem. Eng. J.*, **356**, 492 (2019).
13. A. Dabrowski, Z. Hubicki, P. Podkoscielny and E. Robens, *Chemosphere*, **56**, 91 (2004).
14. P. F. Jahromi, J. Karimi-Sabet and Y. Amini, *Chem. Eng. J.*, **334**, 2603 (2018).

15. Y. H. Kim, H. C. Woo, D. Lee, H. C. Lee and E. D. Park, *Korean J. Chem. Eng.*, **26**, 1291 (2009).
16. J. Liao, H. Li, W. Z. Zeng, D. B. Sauer, R. Belmares and Y. X. Jiang, *Science*, **335**, 686 (2012).
17. J. Kim and M. M. Benjamin, *Water Res.*, **38**, 2053 (2004).
18. G. R. Adelli, S. P. Balguri, P. Bhagav, V. Raman and S. Majumdar, *Drug Deliv.*, **24**, 370 (2017).
19. R. Shang, C. Liu, P. Quan, H. Q. Zhao and L. Fang, *Int. J. Pharm.*, **545**, 163 (2018).
20. S. J. Ahmadi, N. Akbari, Z. Shiri-Yekta, M. H. Mashhadizadeh and M. Hosseinpour, *Korean J. Chem. Eng.*, **32**, 478 (2015).
21. H. S. Li, Y. H. Chen, J. Y. Long, D. Q. Jiang, J. Liu, S. J. Li, J. Y. Qi, P. Zhang, J. Wang, J. Gong, Q. H. Wu and D. Y. Chen, *J. Hazard. Mater.*, **333**, 179 (2017).
22. R. J. Liu, Y. Q. Zhang, J. W. Ding, R. Wang and M. Q. Yu, *Sep. Purif. Technol.*, **174**, 84 (2017).
23. H. S. Lv, Y. P. Sun, M. H. Zhang, Z. F. Geng and M. M. Ren, *Energy Fuel*, **26**, 7299 (2012).
24. M. Coca, S. Mato, G. González-Benito, M. Ángel-Urueña and M. T. García-Cubero, *J. Food Eng.*, **97**, 569 (2010).
25. Z. H. Yu, T. Qi, J. K. Qu and Y. C. Guo, *Hydrometallurgy*, **158**, 165 (2015).
26. W. T. Yi, C. Y. Yan and P. H. Ma, *Desalination*, **249**, 729 (2009).
27. K. Thirugnanasambandham, V. Sivakumar and J. P. Maran, *J. Taiwan Inst. Chem. Eng.*, **46**, 160 (2015).
28. N. N. N. Mahasti, Y. J. Shih, X. T. Vu and Y. H. Huang, *J. Taiwan Inst. Chem. Eng.*, **78**, 378 (2017).
29. P. Abdollahi, J. Karimi-Sabet, M. A. Moosavian and Y. Amini, *Sep. Purif. Technol.*, **231**, 115875 (2020).
30. A. Subasi, B. Sahin and I. Kaymaz, *Int. J. Heat Mass Transfer*, **101**, 295 (2016).
31. Z. Y. Yuan, J. Yang, Y. F. Zhang and X. W. Zhang, *Energy*, **80**, 340 (2015).
32. M. Y. Noordin, V. C. Venkatesh, S. Sharif, S. Elting and A. Abdullah, *J. Mater. Process. Technol.*, **145**, 46 (2004).
33. F. Guesmi, C. Hannachi and B. Hamrouni, *Desalin. Water. Treat.*, **23**, 32 (2010).
34. C. Carvalho, A. Fernandes, A. Lopes, H. Pinheiro and I. Goncalves, *Chemosphere*, **67**, 1316 (2007).

APPENDIX A

Table A1. Multi regression analysis of responses

Source	Sum of squares	df	Mean square	F value	p-Value prob>F	
Total square sum for Y_1						
Mean vs Total	31160.01	1	31160.01			
Linear vs Mean	2050.74	4	512.69	53.26	<0.0001	
2FI vs Linear	21.98	6	3.66	0.32	0.9205	
Quadratic vs 2FI	137.51	4	34.38	6.73	0.0031	Suggested
Cubic vs Quadratic	23.05	8	2.88	0.36	0.9105	Aliased
Residual	48.49	6	8.08			
Total	33441.79	29	1153.17			
Total square sum for Y_1						
Mean vs Total	8.3034	1	8.3034			
Linear vs Mean	0.2067	4	0.0517	54.69	<0.0001	Suggested
2FI vs Linear	0.0014	6	0.0002	0.19	0.9748	
Quadratic vs 2FI	0.0139	4	0.0035	6.68	0.0032	Suggested
Cubic vs Quadratic	0.0022	8	0.0003	0.32	0.9280	Aliased
Residual	0.0051	6	0.0009			
Total	8.5328	29	0.2942			
Model summary statistics for Y_1						
Linear	3.1	0.89	0.88	0.84	356.93	
2FI	3.41	0.91	0.86	0.71	670.82	
Quadratic	2.26	0.97	0.94	0.84	368.88	Suggested
Cubic	2.84	0.98	0.9	−1.42	5515.85	Aliased
Model summary statistics for Y_2						
Linear	0.0307	0.90	0.88	0.85	0.03	Suggested
2FI	0.0344	0.91	0.86	0.71	0.07	
Quadratic	0.0229	0.97	0.94	0.84	0.04	Suggested
Cubic	0.0292	0.98	0.89	−1.47	0.57	Aliased

Table A2. Analysis of variance

Source	Sum of squares	df	Mean square	F value	p-Value prob>F	
Model analysis of variance for A						
Model	2210.22	14	157.87	30.89	<0.0001	Significant
A	34.92	1	34.92	6.83	0.0204	
B	1360.43	1	1360.43	266.19	<0.0001	
C	227.94	1	227.94	44.6	<0.0001	
D	427.45	1	427.45	83.64	<0.0001	
AB	0.36	1	0.36	0.07	0.7946	
AC	9.52	1	9.52	1.86	0.1939	
AD	2.25	1	2.25	0.44	0.5178	
BC	0.00022	1	0.00022	0.000044	0.9948	
BD	0.0529	1	0.05	0.011	0.9204	
CD	9.797	1	9.79	1.92	0.1879	
A^2	1.365	1	1.36	0.27	0.6133	
B^2	34.725	1	34.73	6.79	0.0207	
C^2	65.594	1	65.59	12.83	0.0030	
D^2	9.81	1	9.81	1.92	0.1875	
Residual	71.55	14	5.11			
Lack of fit	61.25	10	6.12	2.38	0.2095	Not significant
Pure error	10.31	4	2.58			
Cor total	2281.77	28				
Model analysis of variance for B						
Model	22.1771	14	1.5841	30.24	<0.0001	Significant
A	0.3745	1	0.3745	7.15	0.0182	
B	13.3774	1	13.3774	255.35	<0.0001	
C	2.4571	1	2.4571	46.90	<0.0001	
D	4.4408	1	4.4408	84.77	<0.0001	
AB	0.0081	1	0.0081	0.15	0.7001	
AC	0.0484	1	0.0484	0.92	0.3528	
AD	0.0361	1	0.0361	0.69	0.4204	
BC	0.0361	1	0.0361	0.69	0.4204	
BD	0.0002	1	0.0002	0.0043	0.9487	
CD	0.0072	1	0.0072	0.14	0.7159	
A^2	0.0268	1	0.0268	0.51	0.4859	
B^2	0.1172	1	0.1172	2.24	0.1569	
C^2	0.8908	1	0.8908	17.00	0.001	
D^2	0.1150	1	0.1150	2.20	0.1606	
Residual	0.7334	14	0.0524			
Lack of fit	0.6158	10	0.0616	2.09	0.2483	Not significant
Pure error	0.1177	4	0.0294			
Cor total	22.9106	28				

APPENDIX B

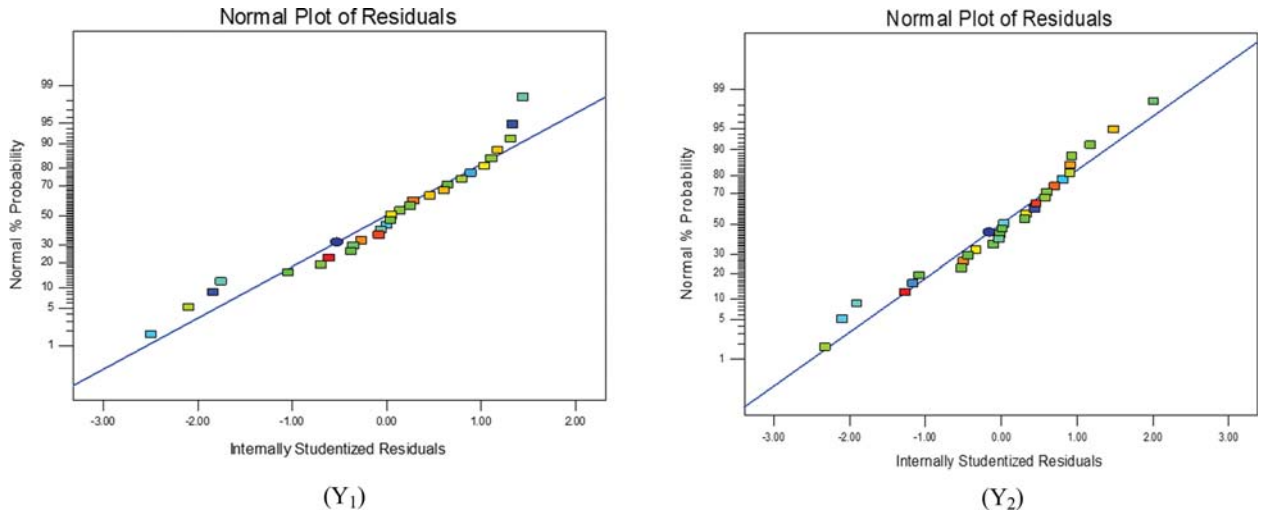

Fig. A1. Residual analysis chart.

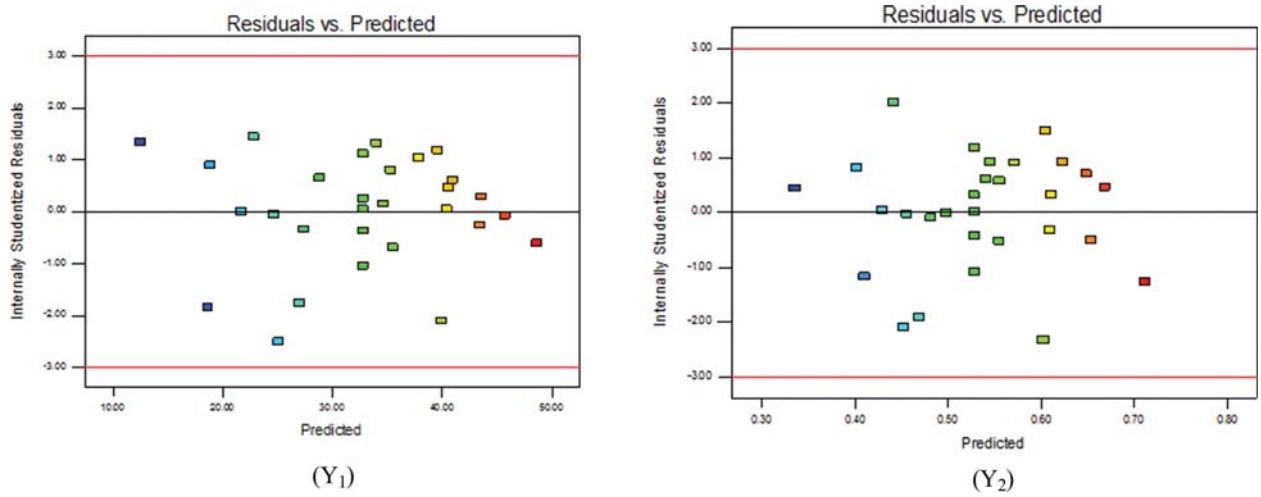

Fig. A2. Residuals vs. predicted.

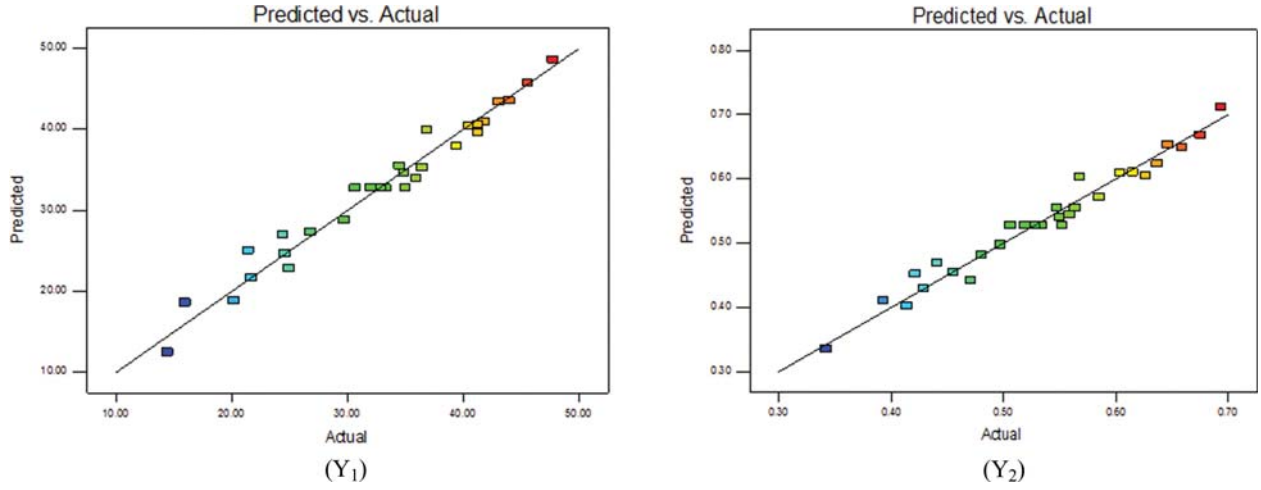

Fig. A3. The comparison of the predicted values to the actual values.